DAVID—a translucent multi-wire transmission ionization chamber for *in vivo* verification of IMRT and conformal irradiation techniques

2006 Phys. Med. Biol. 51 1237

(http://iopscience.iop.org/0031-9155/51/5/013)

INSTITUTE OF PHYSICS PUBLISHING PHYSICS IN MEDICINE AND BIOLOGY

Phys. Med. Biol. **51** (2006) 1237–1248 doi:10.1088/0031-9155/51/5/013

DAVID—a translucent multi-wire transmission ionization chamber for *in vivo* verification of IMRT and conformal irradiation techniques

B Poppe[1], C Thieke[2], D Beyer[1], R Kollhoff[1], A Djouguela[1], A Rühmann[1], K C Willborn[1] and D Harder[3]

[1] WG Medical Radiation Physics, Pius-Hospital and Carl von Ossietzky-Universität, Oldenburg, Germany
[2] Department of Radiation Oncology, Deutsches Krebsforschungszentrum, Heidelberg, Germany
[3] Prof. em. of Medical Physics and Biophysics, Georg-August-Universität, Göttingen, Germany

E-mail: bjoern.poppe@uni-oldenburg.de

Received 12 July 2005, in final form 22 December 2005
Published 15 February 2006
Online at stacks.iop.org/PMB/51/1237

Abstract

Permanent *in vivo* verification of IMRT photon beam profiles by a radiation detector with spatial resolution, positioned on the radiation entrance side of the patient, has not been clinically available so far. In this work we present the DAVID system, which is able to perform this quality assurance measurement while the patient is treated. The DAVID system is a flat, multi-wire transmission-type ionization chamber, placed in the accessory holder of the linear accelerator and constructed from translucent materials in order not to interfere with the light field. Each detection wire of the chamber is positioned exactly in the projection line of a MLC leaf pair, and the signal of each wire is proportional to the line integral of the ionization density along this wire. Thereby, each measurement channel essentially presents the line integral of the ionization density over the opening width of the associated leaf pair. The sum of all wire signals is a measure of the dose-area product of the transmitted photon beam and of the total radiant energy administered to the patient. After the dosimetric verification of an IMRT plan, the values measured by the DAVID system are stored as reference values. During daily treatment the signals are re-measured and compared to the reference values. A warning is output if there is a deviation beyond a threshold. The error detection capability is a leaf position error of less than 1 mm for an isocentric 1 cm × 1 cm field, and of 1 mm for an isocentric 20 cm × 20 cm field.

1. Introduction

Increased quality assurance has been identified as a major prerequisite for the safe application of intensity modulated radiation therapy (Ezzell *et al* 2003). A combination of pre-treatment dosimetric plan verification with increased mechanical and dosimetric constancy checks is state of the art (Ezzell *et al* 2003, Rhein *et al* 2002). *In vivo* dosimetry in IMRT has been performed with TLD detectors (Ling *et al* 1996, Van Esch *et al* 2002), diodes (Higgins *et al* 2003) and MOSFET detectors (Ramaseshan *et al* 2004, Marcie *et al* 2005). However, the reliability of *in vivo* point measurements performed in the high gradient setting of IMRT is subject to question (LoSasso 2003, IMRT Collaborative Working Group 2001). Partridge *et al* (2003) and Spies *et al* (2001) have studied the possibility of beam-profile reconstruction from a portal imaging system, i.e., from information subjected to the influences of photon absorption and scattering in the body of the individual patient.

A desire hitherto not realized has been the permanent monitoring of the photon beam profile during patient treatment by means of a transmission-type radiation detector with spatial resolution, positioned on the *radiation entrance side* of the patient. We have developed a flat, multi-wire ionization chamber to be placed in the accessory holder of the treatment head, with the ability of on-line recording a set of characteristics of the beam profile. The signal from each detection wire is associated with the opening width of one leaf pair of the MLC, and the chamber is constructed from translucent materials in order not to interfere with the light localizing system of the treatment head. With regard to the harp-like arrangement of the detection wires, the new device has been called the DAVID system. However, DAVID also stands for 'device for advanced verification of IMRT deliveries'. The physical arrangement, the measuring properties and the clinical use of the DAVID system are discussed in this paper.

2. Description of the DAVID system

The prototype of the DAVID system has been developed for a standard Siemens linear accelerator (Primus, Digital Mevatron, Siemens Medical Systems, Concord, CA), whose collimating system consists of a pair of opposing jaws moving in the in-plane direction (y-direction) and a MLC with the leaf pairs moving in the cross-plane direction (x-direction). The MLC comprises 29 double-focused leaf pairs. Each of the inner leaf pairs covers a stripe of 1 cm width in the isocentre plane (shortly called ISO plane), while leaf pairs 1 and 29 cover stripes of 6.5 cm width.

The DAVID system is a flat, translucent multi-wire ionization chamber to be placed in the second accessory holder of the linear accelerator. This slot is usually used for physical wedges or blocks, which are not needed for IMRT treatments. The DAVID chamber can either be placed there in exchange for the physical wedges or blocks, or it can be permanently installed at accelerators, which are only used for IMRT. The distance between the nominal photon focus and the plane of the wires is 43.1 cm. The number of detection wires (29 in the case of the used accelerator) equals the number of MLC leaf pairs in the accelerator head.

Figure 1 shows the principal arrangement of detection wires and grounded auxiliary wires within the air-filled volume of the DAVID chamber. Each detection wire of the chamber is positioned exactly on the central projection line of a leaf pair of the MLC collimator. Therefore the distance from one detection wire to the next one is 4.31 mm with a tolerance of 0.1 mm. Ion collection is accomplished by a static electric field between the detection wires and the conducting inner surfaces of the upper and lower cover plates. The conducting layer formed on the cover plates is so thin that the chamber is translucent to the light visor of the localizing system. In order to limit the collecting volume of a detection wire electrostatically, an auxiliary

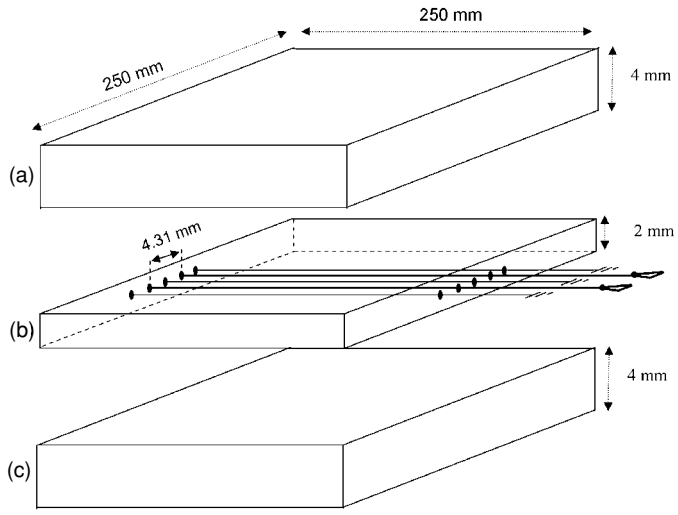

Figure 1. Schematic drawing of the multi-wire ionization chamber in the DAVID system. The blow up sketch illustrates (b) the air-filled collection volume with two of the 29 detection wires connected to the amplifiers and three of the 30 grounded wires, (a) and (c) the 4 mm PMMA cover plates, which carry the translucent chamber voltage electrodes on their inner sides.

wire of the same potential as the detection wires is placed along each midline between two detection wires. An effective collection volume of each measurement wire of 0.03 cm^3 per centimetre of length is obtained with this arrangement.

A potential of +400 V is applied to the electrodes at the inner surfaces of the PMMA cover plates of the chamber, while the detection and auxiliary wires are kept near respectively at ground potential. This polarity was chosen not only to accomplish the saturation of ion collection, but also to prevent the electrons formed by ionization from undergoing gas multiplication in the vicinity of the thin collection wires. These consist of tungsten and have a diameter of 100 μm. In order to provide sufficient secondary electron build-up and mechanical stability of the device, 4 mm was chosen as the thickness of the upper and lower PMMA cover plates.

The detection wires of the DAVID chamber are connected to a multi-channel electrometer (MULTIDOS, PTW-Freiburg). The measurement range of this electrometer is from 60 pA to 10 nA with a resolution of 0.1 pA and a maximum leakage current of 0.1 pA. The charge collected by each detection wire is accumulated on a capacitor. The voltage thereby achieved is read out by the associated amplifier at a rate of 1 s^{-1}. After that the capacitor is instantly reset to zero charge, and a new charge accumulation cycle is started. Additional software is used to control the electrometer taking the readings of all detection wires. In the course of dosimetric plan verification, which is performed once prior to treatment, these readings are stored as patient specific reference values. When the patient is treated in the fractionated treatment course, for each irradiation the actual readings of the detection wires are compared with the reference values. Both the acquisition of the actual readings and the comparison with the reference data are performed immediately during the irradiation of the patient. The only additional time needed to perform an *in vivo* verification is the time for the selection of the patient-specific reference values from the database.

The properties of the DAVID system were explored by a set of experiments whose layout and results are described in the following.

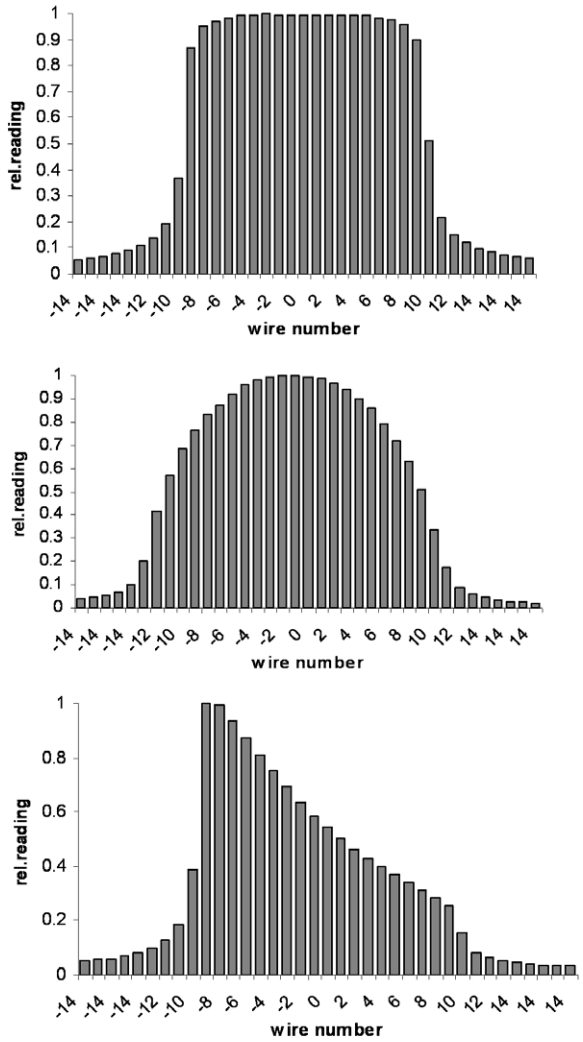

Figure 2. Typical readings of the DAVID chamber for a squared field (10 cm × 10 cm at ISO distance), a circular field (approximately 22 cm diameter at ISO distance) and a virtual wedge field (60 degrees, dose gradient perpendicular to wires) for 6 MV. The abscissa represents the detection wire number (or number of the associated MLC pair) starting at 0 for the central wire. Note that the outer leaf pairs (6.5 cm projected width in isocentre) are controlled by more than one wire.

3. Properties of the DAVID system

3.1. General functioning of the DAVID chamber

In figure 2, the general functioning of the device is illustrated for three typical field forms, a squared, a circular and a virtual wedge field whose dose gradient was perpendicular to the detection wires. Each of the values measured by the multi-channel electrometer represents the ionization signal from a single wire.

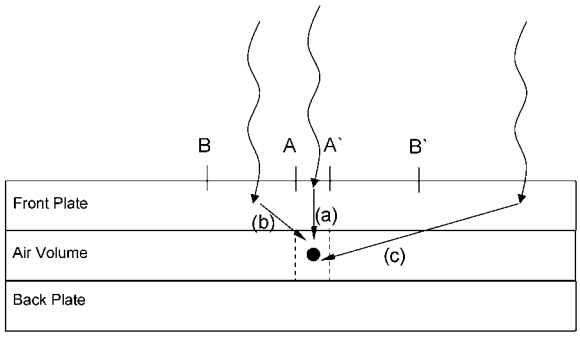

Figure 3. The three groups of secondary electrons contributing to the signal of a measuring wire: (a) secondary electrons originating from the stripe A–A′ of the front plate exposed to photons that have passed the associated leaf pair opening; (b) secondary electrons originating in the front plate from other parts B–A and A′–B′ within the radiation field; (c) secondary electrons originating from parts of the front plate exposed to the collimator leakage radiation. (There are corresponding groups of secondary electrons from the back plate, not drawn here for simplicity.) Dashed lines: borders of the collecting volume.

3.2. Signal interpretation

The reading R_i of each single channel i in terms of ion charge collected is equal to the line integral of the ionization density $I_i(x, y, z)$ of the associated detection wire, where x is the coordinate parallel to the wire and x_1 and x_2 are the wire ends, multiplied by the cross section C of the lengthy collection volume formed along each wire :

$$R_i = \mathrm{C} \int_{x_1}^{x_2} I_i(x, y, z)\, \mathrm{d}x. \tag{1}$$

Approximately (see next paragraph), the integrand $I_i(x, y, z)$ differs from zero only within the interval $[l_{i1}, l_{i2}]$ given by the aperture of the associated leaf pair. Therefore, we have the relationship

$$R_i \approx \mathrm{C} \int_{\mathrm{l_{i1}}}^{l_{i2}} I_i(x, y, z)\, \mathrm{d}x, \tag{2}$$

which indicates the sensitivity of the signal R_i to the aperture of the associated leaf pair.

The signal consists of three components (figure 3): (a) a 'main signal' produced by secondary electrons originating from that part of the front and back plates directly irradiated by photons passing the associated leaf pair opening. (b) a 'scattering signal' due to laterally scattered secondary electrons with an origin in other parts of the front and back plate within the irradiated field and (c) a 'background signal' due to secondary electrons produced by the leakage radiation transmitted through the collimator jaws and MLC leaves.

The 'main signal' of a detection wire can be analysed by varying the opening width of the leaf pair associated with this wire, while keeping all other MLC leaf pairs closed and by subtracting the background signal as measured with fully closed jaws and MLC leaves. The result is shown in figure 4(a): the signal of the selected wire, the 'main signal', increases approximately in proportion with the opening width of the leaf pair. The slight curvature results from the 'over-flattening' of the photon beam due to the effect of the flattening filter. The 'scatter signal', shown in figure 4(b), was analysed by keeping the pair of MLC leaves associated with the selected detection wire closed, while the field size was varied with the help of all other MLC leaf pairs. The result is shown in figure 4(b). The abscissa is the side length

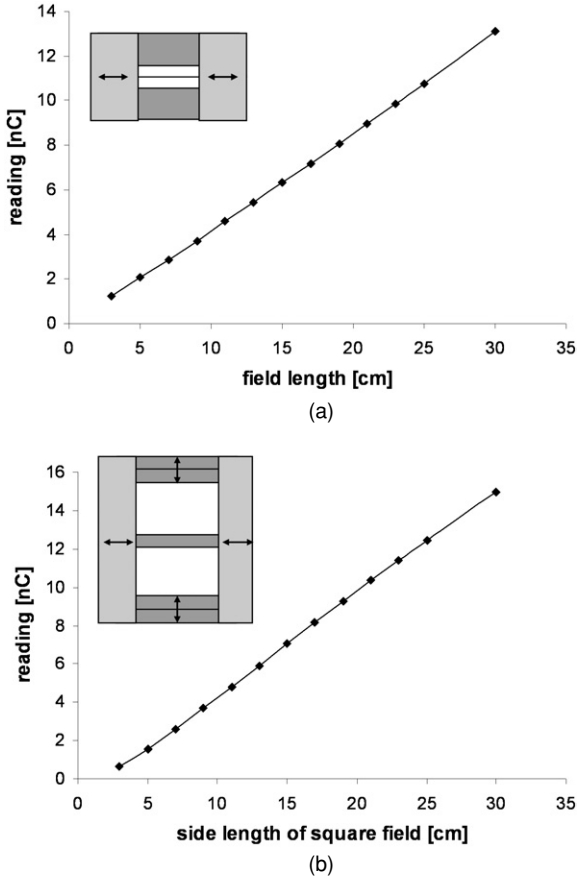

Figure 4. (a) Main signal, i.e., signal from a single wire exposed to the secondary electrons produced by photons, which have passed the opening of the associated leaf pair. (b) Scatter signal, i.e., signal from a single wire exposed to secondary electrons produced by photons from other parts of the radiation field except the stripe determined by the associated leaf pair (see also insets, 6 MV, 50 MU, background signal subtracted).

of a square field whose area was varied. According to this plot, the wire signal increases approximately in proportion with the field side length, and the slight curvature again results from the 'over-flattening'. The proportionality of the signal with the *side length* of the square field, although its *area* was varied, illustrates that the main effect is due to the lateral transport of secondary electrons originating in a close vicinity of the collection wire.

This effect of secondary electrons was further analysed in an additional experiment, in which one leaf pair was opened and the signals of all wires were recorded. According to the profile of the dark columns representing the wire signals in figure 5, the wire positioned directly below the opened leaf pair shows the largest signal, and its neighbour wires show signals of a magnitude decreasing with increasing distance from the open leaf pair. The sum of the signals of all neighbour wires was found to be of a similar magnitude as the signal of the central wire, and the average lateral spread of this profile is about 0.8 cm. When these experiments are performed without the reticle, this profile is an image of the multiple scattering of the secondary electrons originating in the front and back plates and of their lateral transport in the air volume of the DAVID chamber.

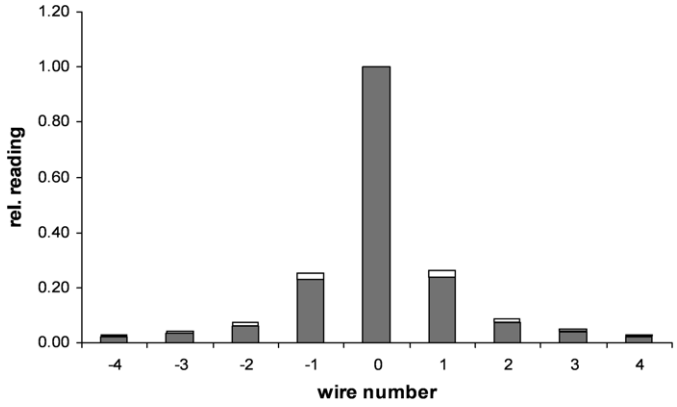

Figure 5. Relative signal distribution of a slit beam 1 cm × 20 cm (6 MV). Due to the laterally scattered electrons, neighbour wires also measure a signal. Bars: measurements without reticle. Additional contributions due to secondary electrons emitted from the reticle are marked as white additions to the dark bars

When these experiments are performed with the reticle in place, which is essentially a PMMA plate of 5 mm thickness positioned about 2 cm upstream of the DAVID chamber, part of the 'main signal' and of the 'scattered signal' is due to secondary electrons originating from the reticle as shown by the white corrections to the dark columns in figure 5. The thickness of the upper plate of the DAVID chamber was chosen in such a way that the sum of the upper plate thickness and the reticle thickness was sufficient to prohibit the entrance of any other secondary electrons into the DAVID chamber, such as secondary electrons from the jaw or MLC collimator, which would blur the signal profile.

3.3. Short time reproducibility of readings

To characterize the short time reproducibility of the readings, a 20 cm × 20 cm and a 1 cm × 1 cm field at 6 MV were irradiated 15 times with a dose of 1 MU and 5 MU. These MU correspond to a dose of 0.007 and 0.04 Gy for the larger and 0.006 Gy and 0.03 Gy for the smaller field size, with the dose referring to 10 cm depth in a RW3 phantom of 15 cm thickness at SSD 90. Pinpoint ionization chamber measurements were carried out at the same time to correct the readings for the small fluctuations of the delivered dose per monitor unit. For 1 MU, the DAVID chamber signals fluctuated by less than 0.025% for field size 20 cm × 20 cm and by less than 3% for 1 cm × 1 cm. For 5 MU, the signal fluctuation was below 0.5%, independent of the field size.

3.4. Collection efficiency

The saturation of the DAVID chamber signal was measured for 6 MV using a prototype of the DAVID chamber in which the chamber voltage could be varied. This measurement was performed at 100 cm focus distance. The radiation pulse duration time was 3 μs. According to the measured saturation curve, the wire signal obtained at 200 V chamber voltage differed from the saturation signal by less then 0.1%. Nevertheless, to ensure to work at the saturation level the commercial version of the DAVID chamber is equipped with a common ionization chamber voltage of 400 V.

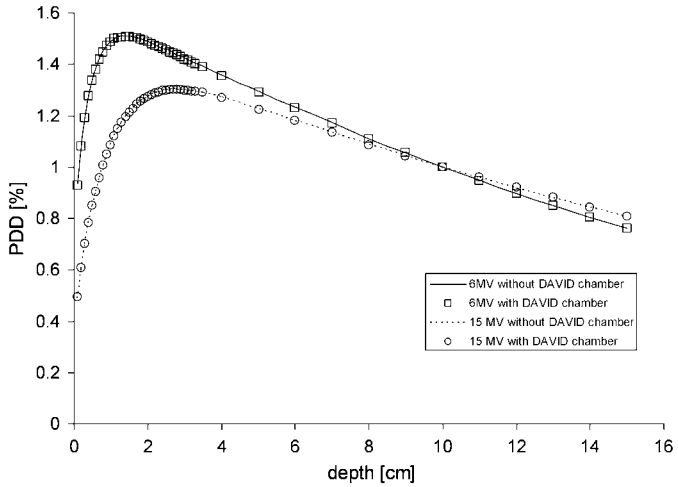

Figure 6. Percentage depth dose curves measured on the central axis with and without the DAVID chamber in the primary beam (6 MV and 15 MV, 10 cm × 10 cm field size at SSD 100)

3.5. Error detection capability

In order to detect a leaf position error, which may occur during patient irradiation, the software is comparing, for each detection wire, the acquired reading with the stored reference value. Any error produced by an imperfect distance between the associated leaves will be detected if the difference between the actual reading and the reference value exceeds a certain limit. The minimal detectable position error is the one that produces a signal difference larger than the inherent fluctuations of the signals. To investigate the minimal detectable position error, we used standard field sizes (1 cm × 1 cm, 3 cm × 3 cm, 10 cm × 10 cm, 20 cm × 20 cm at ISO distance) and studied the relative signal difference between a reference field and faulty fields comprising an artificially induced side length error between 1 mm and 3 mm. The results show that a position error of 1 mm of the associated leaf pair always produces a detectable signal change, because the smallest relative change, 0.61%, was larger than 0.5%, the short time reproducibility.

3.6. Attenuation of the beam by the DAVID chamber

The attenuation of the therapeutic photon beam by a transmission device such as the DAVID chamber should not produce considerable dose rate reductions. Due to the presence of the DAVID chamber in the beam, i.e., of a device with a total thickness of 8 mm PMMA, the dose per monitor unit measured in the isocentre at 10 cm depth in a 15 cm thick RW3 phantom (SSD 90) for a 10 cm × 10 cm at ISO distance was reduced by an attenuation factor of 0.953 ± 0.001 for 6 MV and of 0.968 ± 0.001 for 15 MV. This influence is allowed for by a corresponding correction of the output factor value. The influence on the shape of the relative depth dose curve was studied with 6 MV and 15 MV photon beams at 10 cm × 10 cm field size. There was no detectable influence due to the presence of the DAVID chamber (figure 6) for both energies. Measurements of the relative dose profiles along the main axes with and without the DAVID chamber in the beam did not show deviations larger than 1% for field sizes up to 25 cm × 25 cm (6 MV, SSD 90).

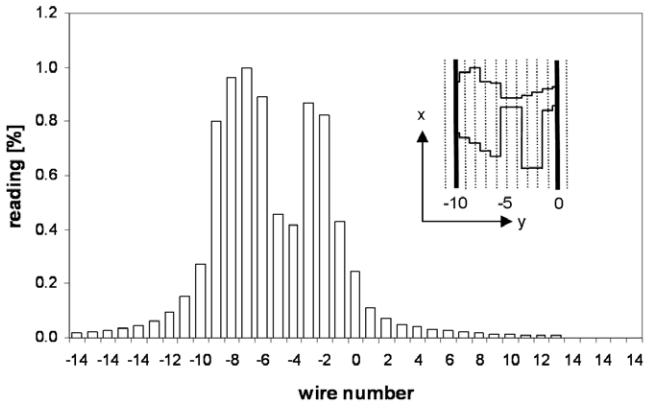

(a)

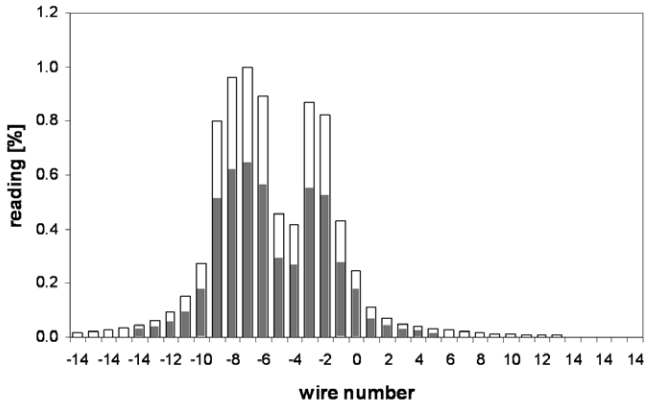

(b)

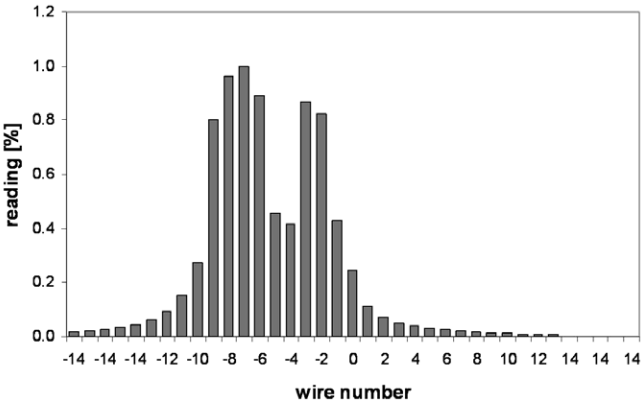

(c)

Figure 7. Example of the *in vivo* verification of a segment of an IMRT field, showing as translucent bars the reference values, which have been defined during treatment planning and have to be attained at the end of the treatment, and as solid bars the values actually accumulated from the start of the irradiation until the moment of observation (a) before the start of the irradiation, (b) after 60% of the dose have been administered and (c) after the end of the irradiation. Inset to (a): field shape of the segment (bold lines: position of the backup jaws, full lines: position of the MLC leaves, dotted lines: positions of the wires)

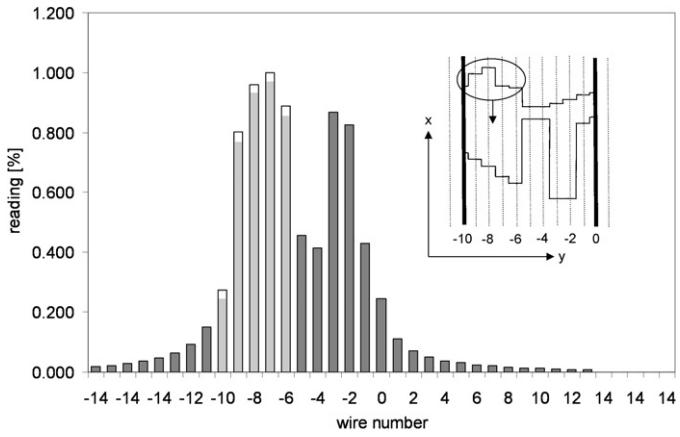

Figure 8. Example of an artificially introduced error, for the IMRT field already referred to in figure 7. The picture shows that for five of the measuring wires the actually measured values did not comply with the reference values due to an error of leaf pair setting. Inset: field shape of the segment, with symbols as in figure 7(a). Encircled: introduced MLC mis-positioning (3 mm).

3.7. Light attenuation by the DAVID chamber

The attenuation of the light field, occurring when the translucent DAVID chamber is placed in the accessory holder of the accelerator, was measured with an illumination meter (Voltcraft DX-200, Conrad Electronics, Hirschau, Germany). The instrument was equipped with a Si photo diode calibrated in Lux. The illumination without the DAVID chamber, measured in the field centre, was 20.6 Lux. Adding the device resulted in an illumination of 17.3 Lux, which was still providing enough light to assure the accurate positioning of the patient. The refraction of light in the front and back plates of the DAVID chamber was estimated to result in a decrease of the light field width by approximately 1 mm for a 40 cm $\times$ 40 cm field.

4. *In vivo* verification with the DAVID chamber

Our concept for the *in vivo* verification of IMRT plans applying the SMLC (step and shoot) method comprises the following steps: for each segment of each field of the IMRT plan, reference values for all wires have to be collected. Most conveniently, this is done during a dosimetric plan verification. The values are stored in a patient specific folder of a database. Since the sensitivity of the DAVID chamber is proportional to air density, the responses of all wires to a standard 40 cm $\times$ 40 cm photon field are also stored.

During the daily treatment of the patient, the software displays the reference values of the wire signals for each segment to be irradiated as translucent bars. To allow for fluctuations of air density, the reference values are corrected up or down in proportion with the wire signals for a standard 40 cm $\times$ 40 cm field recorded beforehand. The wire signals of the DAVID system actually obtained in the administration of a segment to the patient are immediately compared to the reference values (figure 7), while the reference values of the next segment are already loaded by the software of the system.

To test the error detection capabilities, the width of a segment field was modified by an artificially introduced error of -2 mm in a group of leaf pairs. Figure 8 shows the display of the profile of the wire signals after the end of the irradiation. The group of signals, which- fell short of their reference signals by more than 5%, is marked by lighter shading.

5. Discussion and conclusions

We have investigated several features of the DAVID system, a transmission-type ionization chamber with spatial resolution for *in vivo* verification of the photon beam profile, which was developed by our group in cooperation with PTW-Freiburg, Germany. The prototype of this system was developed for a Siemens linear accelerator. Chambers for other accelerators are in preparation. The signal of each wire is proportional to the line integral of the ionization density along this wire. The signal has a main contribution due to secondary electrons from the photons directly hitting the stripe of the field associated with this wire, and it has additional contributions due to secondary electrons set in motion by photons hitting the neighboured stripes within a mean distance of 0.8 cm. The profile of the wire signals is typical for the field shape, e.g., a virtual wedge field profile is directly displayed. Each wire signal increases with the irradiated length of the wire. Position errors of the MLC leaf pairs of 1 mm can be detected by comparison of the wire signals with their reference values, and threshold passing signals can be generated if the difference exceeds a pre-selected value. Variations of air density are allowed for by measuring the wire signal profile for a standard 40 cm $\times$ 40 cm field each morning and applying the appropriate daily software correction. A general feature of the DAVID system is that the sum of all wire signals, proportional to the dose-area product across the photon beam, is a measure of the total radiant energy administered to the patient at the given acceleration potential, 6 or 15 MV. Furthermore, the dose-area product has to be regarded as a most useful parameter especially of narrow photon beams (Djouguela *et al* 2006).

Regarding patient treatment verification of IMRT deliveries, most centres perform dosimetric pre-treatment verification of the treatment fields, be it on a single field or on a total plan procedure. During the actual treatment, the primary focus is on patient positioning rather than dosimetry. *In vivo* dosimetric techniques in conformal radiotherapy are widely used by measuring the entrance dose inside the radiation field. Several groups have implemented these techniques for IMRT techniques using TLD, diode or MOSFET detectors. The obvious drawback of these methods is the only pointwise verification of the delivered doses. Spies *et al* (2001) and Partridge *et al* (2003) describe the concept and a proof-of-principle experiment for *in vivo* verification of intensity modulated photon fields using a flat panel EPID in combination with a three-dimensional reconstruction algorithm. By applying an iterative phantom-scatter estimation technique and inverse attenuation corrections, the signal measured by the EPID is then converted into the primary photon fluence profile. Hence, the accuracy of the reconstructed signal which will be used for further comparisons strongly depends on how exactly the recalculation of the absorption and scattering in the patient can be performed. Considering daily fluctuations in patient position, small errors of MLC positioning in the millimeter range will hardly become detectable. On the other hand, the *in vivo* verification of the photon fluence profile by spatially resolved monitoring of the beam on the radiation entrance side of the patient, as here described for the DAVID chamber, has the advantage of measuring an undisturbed signal, which is solely related to machine dependent parameters.

This device has been produced as two prototypes, which were wire-connected to the multidos electrometer system (PTW-Freiburg). Present efforts have led to a wireless modification, which can more easily be positioned in the accelerator head. The response of the clinical staff to this new equipment has been very positive, especially since the immediate visual comparison between the actual profile of the wire signals and the reference profile is permanently provided during the full time of patient treatment. The gap between intensified constancy checks and pre-treatment dosimetric IMRT plan verification is closed by the proposed method of collecting reference values of the DAVID system during dosimetric plan verification and performing a daily *in vivo* verification of the single segments.

As mentioned above, threshold passing signals will indicate that a predefined dose difference has been exceeded. Two of these threshold passing levels can be set individually for each patient: a 'warning level', indicating moderate deviations (e.g. 3% signal differences); and an 'alarm level' (e.g. 5%) indicating major differences. We recommend a more detailed analysis of the deviations if an individual leaf pair has exceeded the alarm level during several irradiations.

In this work the DAVID chamber has been used in connection with the step-and-shoot or SMLC technique. The potential applicability for dynamic techniques has also been accounted for in the design of the system and will be evaluated in future work.

References

Djouguela A, Harder D, Kollhoff R, Rühmann A, Willborn K C and Poppe B 2006 The dose-area product, a new parameter for the dosimetry of narrow photon beams *Z. Med. Phys.* **16** submitted

Ezzell G A, Galvin J M, Low D, Palta J R, Rosen I, Sharpe M B, Xia P, Xiao Y, Xing L and Yu C X 2003 Guidance on delivery, treatment planning, and clinical implementation of IMRT: report of the IMRT subcommittee of the AAPM radiation therapy committee *Med. Phys.* **30** 2089–115

Higgins P D, Alaei P, Gerbi B J and Dusenbery K E 2003 *In vivo* diode dosimetry for routine quality assurance in IMRT *Med. Phys.* **30** 3118–23

Intensity Modulated Radiation Therapy (IMRT) Collaborative Working Group 2001 Intensity modulated radiotherapy: current status and issues of interest *Int. J. Radiat. Oncol. Biol. Phys.* **51** 880–914

Jornet N 2004 *In vivo* diode dosimetry for quality assurance in IMRT *Med. Phys.* **31** 1642–3

Ling C C, Burman C, Chui C S, Kutcher G J, Leibel S A, LoSasso T, Mohan R, Bortfeld T, Reinstein L, Spirou S, Wang X H, Wu Q, Zelefsky M and Fuks Z 1996 Conformal radiation treatment of prostate cancer using inversely planned intensity modulated photon beams produced with dynamic multileaf collimators *Int. J. Radiat. Oncol. Biol. Phys.* **35** 721–30

LoSasso T J 2003 Quality assurance of IMRT *A Practical Guide to Intensity Modulated Radiation Therapy* (Madison, WI: Medical Physics Publishing) pp 147–67

Marcie S, Charpiot E, Bensadoun R J, Ciais G, Herault J, Costa A and Gerard J P 2005 *In vivo* measurements with MOSFET detectors in oropharynx and nasopharynx intensity-modulated radiation therapy *Int. J. Radiat. Oncol. Biol. Phys.* **61** 1603–6

Partridge M, Ebert M and Hesse B M 2003 IMRT verification by three-dimensional dose reconstruction from portal beam measurements *Med. Phys.* **29** 1847–58

Ramaseshan R, Kohli K S, Zhang T J, Lam T, Norlinger B, Hallil A and Islam M 2004 Performance characteristics of a microMOSFET as an *in vivo* dosimeter in radiation therapy *Phys. Med. Biol.* **49** 4031–48

Rhein B, Häring P, Debus J and Schlegel W 2002 Dosimetric verification of IMRT treatment plans at the German Cancer Center *Z. Med. Phys.* **12** 122–32 (in German)

Spies L, Partridge M, Groh B A and Bortfeld T 2001 An iterative algorithm for reconstructing incident beam distributions from transmission measurements using electronic portal imaging *Phys. Med. Biol.* **46** N203–11

Van Esch A, Bohsung J, Sorvari P, Tenhunen M, Paiusco M, Iori M, Engstrom P, Nystrom H and Huyksens D P 2002 Acceptance tests and quality control (QC) procedures for the clinical implementation of intensity modulated radiotherapy (IMRT) using inverse planning and the sliding window technique: experience from five radiotherapy departmens *Radiother. Oncol.* **65** 53–70